



Characterizing pozzolanic activity of rice husk ash by impedance spectroscopy

S. Wansom^{a,*}, S. Janjaturaphan^a, S. Sinthupinyo^b

^a National Metal and Materials Technology Center, 114 Phahonyothin Rd., Klong 1, Klong Luang, Pathumthani 12120, Thailand

^b Siam Research and Innovation Co., Ltd., 51 Moo 8, Tubkwang, Kaeng Khoi, Saraburi 18260, Thailand

ARTICLE INFO

Article history:

Received 10 March 2010

Accepted 17 August 2010

Keywords:

Amorphous material (B)

Pozzolan (D)

Impedance spectroscopy (B)

Characterization (B)

ABSTRACT

Rice husk ash (RHA) has long been known to possess a pozzolanic property. The abundance of rice husk as agricultural waste makes RHA the most promising candidate to be used as a supplementary cementitious material (SCM) in many rice-exporting countries. The use of RHA as an SCM helps reduce the use and thus the production of cement that involves great energy consumption and CO₂ emission. To promote the use of RHA as an SCM, a method to assess its pozzolanic activity is needed for the process of optimizing the burning conditions and/or selecting RHA from uncontrolled burning of rice husk as biomass fuel.

The present work aims to use impedance spectroscopy to characterize pozzolanic activity of RHAs prepared on a pilot scale. The method is based on the rate of the normalized conductivity change of the Ca(OH)₂ + RHA paste, $d(\sigma/\sigma_0)/dt$, during the first 24 h of hydration. The measurement was found to be sensitive to the unburnt carbon content in the 6–8 wt.% range and the amorphous SiO₂ content (regardless of the unburnt carbon content). When used to evaluate two separate groups of RHAs, each with comparable unburnt carbon contents, the method gives very high correlation coefficients to the strength activity index at 3, 7, and 28 days. However, the correlation coefficients fall significantly when RHAs with vast difference in the unburnt carbon contents are considered together. The method thus proves to be powerful for evaluation of the pozzolanic activity of RHAs with comparable carbon contents.

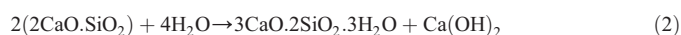
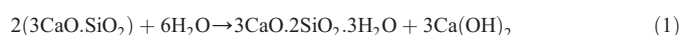
© 2010 Elsevier Ltd. All rights reserved.

1. Introduction

Production of ordinary Portland cement (OPC) requires a lot of energy (~1.7 MJ/kg [1]) and produces an enormous amount of carbon dioxide emission (~1 ton CO₂/1 ton cement [2]) compared to other industries. The energy crisis and global warming awareness have currently caused many cement manufacturers and construction companies to partially replace OPC with other supplementary cementitious materials (SCM) in order to reduce the use and hence the production of OPC. Many of these materials are industrial by-products, such as fly ash (from burning coal in power plants), silica fume (from silicon industry), blast furnace slag (from iron and steel production), and rice husk ash or RHA (from rice mills). Partial incorporation of these industrial by-products as SCM is thus a “constructive” solution to not only help save energy and reduce the cause of global warming, but also to decrease the amount of industrial wastes at the same time. When used appropriately, these materials can also improve compressive strength of cement-based products due to their unique pozzolanic property, i.e., providing reactive SiO₂ to

react with water and Ca(OH)₂ that forms from the hydration of calcium silicates in cement (Eqs. (1) and (2)), to yield calcium silicate hydrate, which is responsible for the strength in cement-based materials.

Hydration reactions [3]:



For many rice-exporting countries such as Thailand, Vietnam, and India, the abundance of rice husk makes RHA the most promising material to be re-utilized as an SCM.

In Thailand, the world's leading rice-exporter alone, the annual production of approximately 7 million tons of rice husk would result in about 1.6 million tons of RHA [4]. Unfortunately, most of this rice husk is usually burnt at temperatures in excess of 1000 °C as biomass fuel for boilers. This process results in vast amounts of poor-quality RHA being discarded in landfills, causing environmental and health-related problems to nearby communities. Burning rice husk at such high temperatures causes amorphous SiO₂, the rich and chemically reactive species in the husk, to turn into its high-temperature crystalline form called cristobalite that weakens the pozzolanic activity of the resulting RHA. Furthermore, prolonged or substantial exposure to respirable cristobalite is known to cause a serious lung disease called silicosis. These problems can be greatly alleviated if rice

* Corresponding author. Tel.: +6 2564 6500x4042.

E-mail address: supapowr@mtec.or.th (S. Wansom).

husk is burnt under appropriate conditions and the resulting RHA can be used in large volumes as an SCM.

Although the use of RHA in concrete was patented in 1924 [5], it was not until the 1970s that researchers started to utilize RHA produced from controlled combustions. The pioneering work of Mehta [6] stated that in order to maximize the amorphous SiO_2 content in RHA for pozzolanic applications, rice husk should be incinerated by maintaining the temperature in the vicinity of 500 °C for a prolonged duration, on the order of days. However, such prolonged incinerating duration is inappropriate for industrial-scale incineration. To enhance the use of high-quality RHA as an SCM, a method to assess its pozzolanic activity is needed for the process of optimizing the incinerating conditions (e.g., temperature, duration, O_2 flow, prior treatments, etc.) and/or selecting RHA which results from uncontrolled burning of rice husk as biomass fuel.

The main factors constituting good pozzolanic activity of RHA as identified in the literature include small particle size [7], low unburnt carbon content [8], high specific surface area [9], and, most importantly, high amorphous SiO_2 content [9]. In addition to increasing the specific surface area, the small RHA particle size, preferably less than the median cement particle size of 10 μm , may also help improve the compressive strength of the product through the so-called packing effect of fine particles in between the cement particles, hence providing a finer pore structure [10]. Mechanical grinding is thus usually adopted after the incineration to improve the pozzolanic activity of RHA. These factors are, however, not necessarily correlated. Some RHA may contain a high amorphous SiO_2 content, but with low specific surface area [11] or with high unburnt carbon content [8]; some may show a high specific surface area as a result of high unburnt carbon content [7]. It is, therefore, difficult to evaluate the pozzolanic activity of RHA by considering each of these factors independently.

Several methods to evaluate the pozzolanic activity of different pozzolans (not necessarily RHA) have been proposed in the literature. The accelerated chemical method [12], where the amount of $\text{Ca}(\text{OH})_2$ consumed in the reaction with a pozzolan is measured, proves to be the most direct as well as the most complicated method. The most widely used method, although the most time-consuming and most indirect, is the strength activity index method. It compares the compressive strengths of cement mortars with and without a pozzolan in percentage terms, according to ASTM C311 [13]. The amount of amorphous SiO_2 (also called soluble silica) as determined by several chemical extraction methods has also been used as an indicator for the pozzolanic activity. The “silica activity index”, proposed by Mehta [6], is calculated from the percentage of SiO_2 dissolved in boiling 0.5 M NaOH solution after 3 min of extraction. The Spanish Standards [14,15] specify extracting the amorphous SiO_2 by HCl acid and boiling 4 M KOH solution for 4 h. Payá et al. [9] proposed a rapid analytical method that involves titrating the RHA/glycerol solution with an aqueous glycerol solution of barium hydroxide. Although the method could be completed in less than an hour, their results were found to be in good agreement with those obtained from the standard method. The disadvantages of these chemical extraction methods are that they either are tedious or require careful analytical skills as stages of filtration and/or titration are involved.

A number of conductometric methods, where the pozzolanic activity is indirectly measured by monitoring the change in electrical conductivity when $\text{Ca}(\text{OH})_2$ reacts with a pozzolan, were proposed by several authors. These methods all rely on the fact that the consumption of Ca^{2+} and OH^- by the pozzolanic reaction leads to the decrease in conductivity of the $\text{Ca}(\text{OH})_2$ + pozzolan mixture as the reaction proceeds over time. Hence, the faster the conductivity drops, the higher is the pozzolanic activity. Based on direct current (DC) measurements, Luxán et al. [16] studied the conductivity change when natural rock pozzolans reacted with saturated $\text{Ca}(\text{OH})_2$ solution at 40 °C. The conductivity change during the first 2 min, $\Delta\sigma$ (mS/cm),

allowed a broad classification of the pozzolans into three groups, including non-pozzolanicity ($\Delta\sigma < 0.4$), variable pozzolanicity ($0.4 \leq \Delta\sigma \leq 1.2$), and good pozzolanicity ($\Delta\sigma > 1.2$). Tashiro et al. [17] evaluated the pozzolanic activities of various pozzolans by monitoring the changes in electrical resistivity (the reciprocal of conductivity) during the first 72 h after the pozzolans were mixed with $\text{Ca}(\text{OH})_2$ and water in form of a paste. Measured under steam curing at 70 °C and using a 1.02 kHz alternating current (AC), the rise in resistivity of the pastes agreed well with $\text{Ca}(\text{OH})_2$ consumption as studied by X-ray diffraction (XRD). However, since the measurements were made under elevated-temperature steam curing, the investigation does not provide information on the reaction rate at ambient temperatures. Most recently, Payá et al. [18] proposed an enhanced conductivity technique for evaluation of fly ash pozzolanic activity. The pozzolanic activity was quantified in terms of the relative loss in conductivity at 100, 1000, and 10 000 s reaction times.

Building on the success of monitoring cement setting and hardening via electrical impedance methods, McCarter and Tran [19] measured the AC conductivity change of various pozzolans (not including RHA) mixed with $\text{Ca}(\text{OH})_2$ powder and water to form a paste for ~48 h, at a fixed frequency of 5 kHz. This frequency was believed to be sufficiently high to overcome polarization effects at the electrodes that were normally encountered in DC or low-frequency AC measurements. The maximum rate of change of conductivity and the time at which it occurred were employed to rank the pozzolanic activity of the materials. Their results, however, did not completely agree with the pozzolanic activity as examined by an accelerated lime consumption test.

The present work aims to use impedance spectroscopy to characterize the pozzolanic activity of different RHAs prepared on a pilot scale (~100 kg RHA/h capacity). The technique involves passing AC excitation of set amplitude over a range of frequency through the sample in order to measure its current response. The ratio of the applied voltage and the current response is the complex impedance, which is a function of the frequency at which the voltage is applied. The conductivity is then extracted from the real part of the complex impedance value. The AC conductivity change of the $\text{Ca}(\text{OH})_2$ + RHA pastes as a result of the pozzolanic reaction is followed for about 2 days. The rate of change of conductivity is discussed with respect to the strength activity indices and other physical properties known to influence the pozzolanic activity of the RHA.

2. Experimental methods and materials

Six types of RHA prepared from rice husk of the same source were investigated. The husk was incinerated under either combustion (with excess O_2 , denoted COM) or gasification (with limited O_2 , denoted GAS) conditions for 30 min, at three different temperatures of 600 °C, 750 °C, and 900 °C. Each of the resulting RHA was milled to obtain a mean particle size of ~10 μm as confirmed by the particle size distribution (Mastersizer S, Malvern Instrument, UK) in Fig. 1. The milled RHA was used in the analyses throughout this work. The specific surface area of each RHA was investigated by nitrogen adsorption (Autosorp-1, Quanta Chrome, USA) after being outgassed at 300 °C for 6 h. The phasal composition of the RHA was studied by X-ray diffraction (XRD, JEOL, JDX 3530, 2 kW, Japan) while the oxide composition was examined by X-ray fluorescence spectroscopy (XRF, Phillips, PW 2404, 4 kW, Netherlands) using boric acid as a binder at a RHA:boric acid ratio of 3:1.25 by weight. Since XRF is incapable of detecting such light atoms as carbon, the unburnt carbon content of the RHA was measured by a CHNS/O analyzer (TruSpec CHN, LeCO, UK). The LOI was determined from the weight loss of the RHA when ignited to constant mass at 800 °C, in accordance with ASTM C311. Following the variation to the Spanish standard methods [14,15] proposed by Payá et al. [9], the amorphous SiO_2 content was

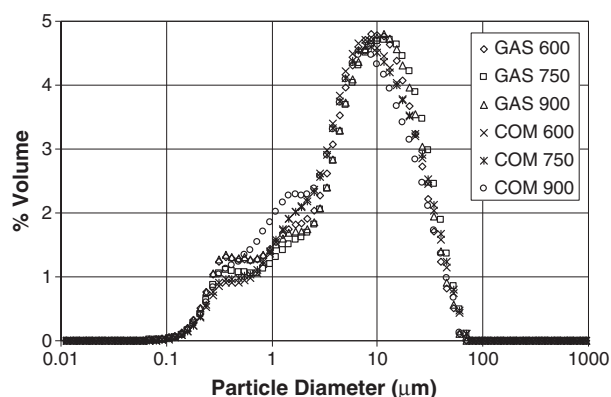


Fig. 1. Particle size distribution of the RHAs.

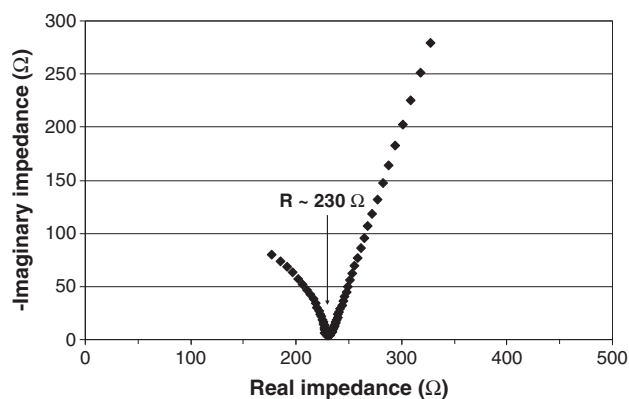


Fig. 3. An example of a Nyquist plot taken from the paste of GAS 600 at $t = 10$ h.

determined from the weight loss of the RHA sample after being dissolved in a boiling 4 M KOH solution for 3 min.

For the impedance measurements, each RHA was mixed with $\text{Ca}(\text{OH})_2$ powder (98.0%, VWR International, England) and drinking water (Sprinkle, M. Water, Thailand) to form a paste at a fixed RHA: $\text{Ca}(\text{OH})_2$ ratio of 9:1 and a water:solid ratio of 9:10. The ratios were adopted to compensate for the high water absorption of the RHA, to ensure a castable consistency of the pastes. The use of a fixed water:solid ratio was to control for the influence of water content on the overall conductivity to be essentially constant for all pastes. The pastes were cast into a 25 mm \times 25 mm \times 25 mm polycarbonate mold, with a pair of stainless steel electrodes (24 mm \times 38 mm \times 1 mm) inserted as shown in Fig. 2. The top surface of the paste was sealed with a piece of polycarbonate to prevent carbonation of the $\text{Ca}(\text{OH})_2$ solution. The impedance measurements were made using an Autolab PGSTAT302 (ECO CHEMIE, The Netherlands) with frequency ranging from 1 MHz to 1 Hz, and a fixed amplitude of 0.35 V, with no bias. Noting the time when water was added to the solid mixture at $t = 0$, the measurements were made every 15 min starting from ~ 5 min for about 2 days under room temperature (25 $^\circ\text{C}$) in a 100% relative humidity chamber. For each run, the impedance data were plotted in a Nyquist fashion (real vs. negative imaginary impedance) and the real impedance value at the cusp (where the imaginary impedance was closest to zero) was taken as the resistance of the paste at that specific time. For instance, the resistance at $t = 10$ h of the GAS 600 paste, as shown in Fig. 3, is approximately 230 Ω . The resistance, R , at each time was converted to the conductivity, σ , using the length, L , and cross-sectional area, A , of the sample following the relationship: $\sigma = L/(RA)$. The change in conductivity of the paste

as a function of hydration time was used to assess the pozzolanic activity of the RHA.

To corroborate the results from conductivity measurements, the amount of $\text{Ca}(\text{OH})_2$ remaining in the pastes were studied by thermal analysis. Thermogravimetry (TG) and derivative thermogravimetry (DTG) analyses were performed on the pastes prepared exactly the same way as for the conductivity measurements but having been hydrated for only 16 h in the same environment. The analyses were made from 30 $^\circ\text{C}$ to 1000 $^\circ\text{C}$ at a heating rate of 10 $^\circ\text{C}/\text{min}$ in a 20 ml/min N_2 atmosphere. Since all the samples initially contain the same amount of $\text{Ca}(\text{OH})_2$, the less amount remaining (i.e., the more amount consumed) should signify higher pozzolanic activity of the RHA.

The strength activity indices at 3, 7, and 28 days were obtained from cement mortars with 10% RHA replacement (by weight of cement) according to ASTM C109 [20] for blended cements. The water-to-solid ratios for each mortar were tailored to obtain a fixed flow of 110 ± 5 from a flow table test. This procedure compensates for the different amounts of water absorbed by the different RHAs in order to reduce the influence of any structural defects resulting from the decreased workability (due to the increased viscosity of the pastes containing RHA with high water absorption) on the compressive strength. The reported strength activity index is an average of three replicates for each RHA sample.

3. Results and discussion

Table 1 shows the physical properties of the RHAs. The compressive strengths of mortars with 10% RHA replacement under fixed flow condition, corresponding to the strength activity indices in Fig. 4, are also presented at the bottom of the table. Although the mean particle sizes of all the RHAs were controlled to be approximately the same ($\sim 10 \mu\text{m}$) by milling, a vast difference in the measured specific surface area is still observed. For a fixed incinerating temperature, RHAs from gasification process seem to have higher specific surface area than their combustion counterparts. This difference might be explained by considering the unburnt carbon contents in Table 1, which are always higher for RHAs in the GAS series than the COM series, given the same burning temperature. The cause of this difference is that the amount of oxygen provided for the gasification process is insufficient to convert all organic carbon to CO_2 completely, thus leaving a higher unburnt carbon content in the RHAs than in the combustion process. According to Nehdi et al. [7], the unburnt carbon from the incineration of rice husk exhibits very high specific surface area ($\sim 1000 \text{ m}^2/\text{g}$) owing to its microporous structure. Hence, the high specific surface area in the GAS series may be due to the high carbon content, which would adversely affect the pozzolanic activity despite the high specific surface area. Consequently, the systematic increase in the specific surface area (from right to left in Table 1) is not necessarily associated with a systematic increase in the

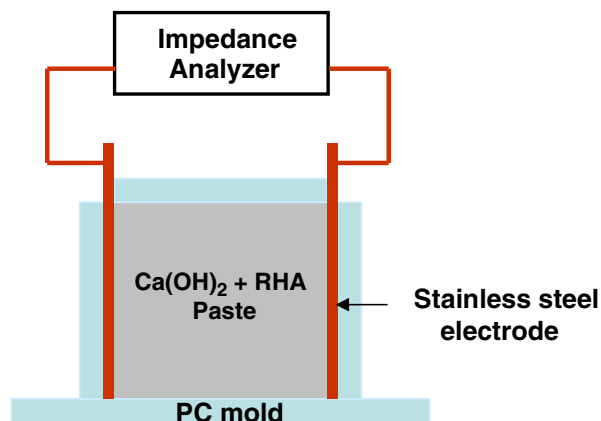


Fig. 2. Experimental setup for the electrical impedance measurements.

Table 1
Physical properties of the RHAs.

	GAS 600	GAS 750	GAS 900	COM 600	COM 750	COM 900
Mean particle size (mm)	9.24	11.01	9.69	9.92	10.05	8.83
Specific surface area (m ² /g)	287.13	160.00	126.03	104.50	48.69	9.57
Chemical oxide composition (wt.%)						
SiO ₂	91.39	93.14	93.59	93.02	92.12	93.22
Al ₂ O ₃	1.22	0.68	0.89	0.69	0.78	0.70
Fe ₂ O ₃	0.34	0.30	0.31	0.28	0.28	0.27
CaO	4.12	2.94	2.28	3.03	3.94	2.81
MgO	0.64	0.61	0.61	0.69	0.69	0.65
SO ₃	0.22	0.22	0.21	0.20	0.19	0.17
Na ₂ O	–	–	–	–	–	0.19
K ₂ O	1.16	1.24	1.30	1.22	1.14	1.16
P ₂ O ₅	0.84	0.80	0.82	0.80	0.78	0.76
MnO	0.08	0.07	–	0.07	0.08	0.07
Equivalent alkalis (Na ₂ O + 0.658K ₂ O)	0.76	0.82	0.86	0.80	0.75	0.95
LOI (wt.%)	11.10	9.37	10.70	4.06	2.39	1.15
Unburnt carbon (wt.%)	5.58	5.88	7.49	0.69	0.38	0.47
Amorphous SiO ₂ (wt.%)	83.81	82.27	62.38	90.94	85.38	38.77
Compressive strength (MPa) (mortar with 10% RHA, fixed flow condition)						
3 days	28.15	27.07	24.91	26.87	26.09	24.61
7 days	40.31	41.19	37.07	39.32	38.74	36.48
28 days	54.72	56.58	51.39	54.52	55.80	52.07

compressive strength at all ages considered, contradicting the previous finding by Payá et al. [9]. Moreover, the RHAs with low carbon contents (the COM series) do not necessarily yield higher compressive strengths than the ones with higher carbon contents (the GAS series), at a fixed burning temperature. This is in contrast to the previous finding by Nair et al. [8] who observed that RHAs with lower carbon content (as measured by LOI) led to improved pozzolanicity (as measured by the conductometric method of Luxán et al. [16]) and higher mortar compressive strength. Even when the LOI is considered, the correlation between low LOI and high compressive strength is still not evident in the present work.

The oxide composition, as determined by XRF, in Table 1 shows very similar SiO₂ contents for all RHAs. However, since XRF cannot differentiate the various phases of SiO₂, these numbers reflect not only the amorphous SiO₂ content, but also its crystalline forms, e.g.,

cristobalite and quartz. The presence of these crystalline phases of SiO₂ is confirmed by the XRD patterns in Fig. 5. Considering only the amorphous SiO₂ contents (from chemical extraction) in Table 1, GAS 900 and COM 900 exhibit the lowest amorphous SiO₂ content in their respective series, in agreement with their highest cristobalite peaks ($2\theta \sim 22^\circ$) in the series in Fig. 5. These two RHAs thus show the lowest mortar compressive strength at all ages in their series, a result similar to that reported by Payá et al. [9]. Nevertheless, it should be noted that despite their vast difference in the amorphous SiO₂ contents, GAS 900 and COM 900 still exhibit approximately the same compressive strengths at all ages and that, among the six RHAs, the highest amorphous SiO₂ content in COM 600 does not necessarily lead to the highest compressive strength at any of the ages considered. The XRD patterns of the RHAs burnt at lower temperatures (600 °C and 750 °C) only show diffuse peaks centered about $2\theta \sim 22^\circ$, which are characteristic of amorphous SiO₂. The presence of crystalline SiO₂, at the expense of amorphous SiO₂, as the burning temperature increases, as shown in Table 1, is also in agreement with the work of Mehta [6]. The 3-day compressive strength also increases with decreasing burning temperature, similar to the trend for the amorphous SiO₂ content and the specific surface area. Moreover, for a given burning temperature, RHAs in the GAS series tend to yield higher 3-day compressive strength than the COM series, similar to the trend for the specific surface area and the unburnt carbon content. However, as the mortars were aged longer to 28 days, the RHAs burnt at 750 °C become the ones that give the highest compressive strength for both the COM and GAS series, and, for a fixed burning temperature, the GAS series no longer exhibits significantly higher compressive strength than the COM series.

The presence of quartz detected in all RHAs in Fig. 5 might result from some contamination by sand from rice fields, as suggested by Jaubertie et al. [21], since it does not seem to have any relationship with the burning temperature. On the contrary, the amount of calcite (CaCO₃) in Fig. 5 seems to decrease with increasing burning temperature for both the COM and GAS series. This trend might be explained by the decomposition of calcite, usually occurring between 520 °C and 730 °C [22], which proceeds to a greater extent as the temperature increases.

The above observations suggest that the pozzolanic activity of the RHA, as reflected by the mortar compressive strength or the strength activity index to some extent, cannot be assessed by considering any

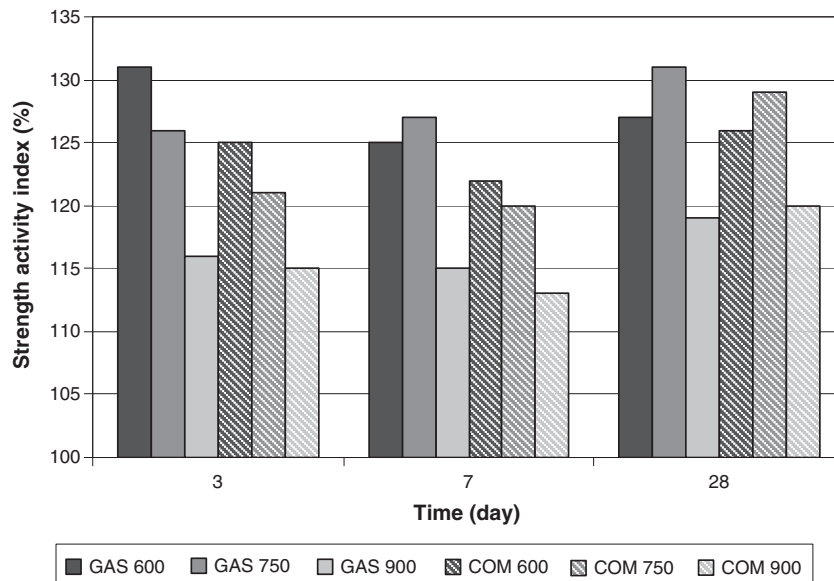


Fig. 4. Strength activity indices of mortars with 10% RHA replacement under fixed flow condition. The calculations are based on the plain mortar compressive strengths of 21.48, 32.36, and 43.25 MPa at 3, 7, and 28 days, respectively.

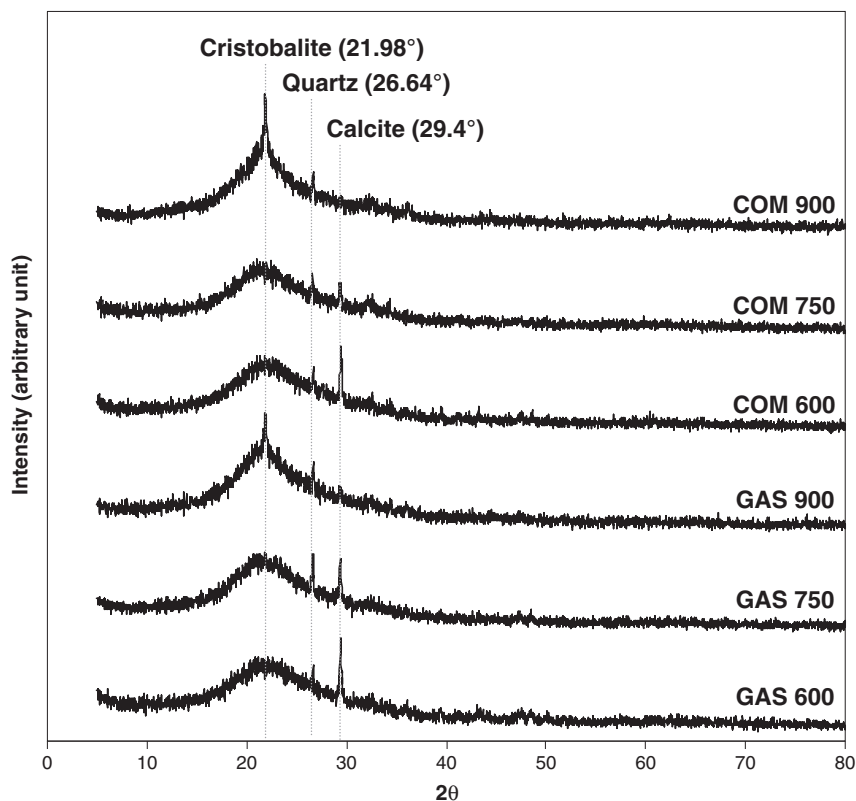


Fig. 5. X-ray diffraction patterns of the RHAs.

of these physical properties separately. The present work thus aims to measure the pozzolanic activity of the RHA from the change in AC conductivity of the $\text{Ca}(\text{OH})_2$ + RHA pastes, treating the conductivity change as a combined effect of all these physical factors; the results are as shown in Fig. 6. It should be stressed that although the present work and the work of McCarter and Tran [19] are similar with respect to the use of impedance spectroscopy to characterize pozzolanic activity, our methods for arriving at the AC conductivity are quite different. While McCarter and Tran [19] relied on the conductivity at a fixed frequency of 5 kHz, believed to be able to reduce the contributions from the electrode polarization effects, the present work does not assume a fixed frequency for the conductivity measurements. Instead, the resistance was taken from any frequency that gives the lowest imaginary impedance in absolute value (i.e., where the capacitance contributions are most negligible). The authors believe that this method, along with the use of high-frequency AC excitation, will effectively reduce the contributions from both the double layer capacitance and the polarization resistance at the electrolyte/electrode interfaces. The measured conductivity change should then be truly indicative of the pozzolanic activity.

Fig. 6a shows the change in conductivity derived from the impedance measurements. To account for the conductivity contributions from the unburnt carbon and other soluble salts in the RHA, the conductivity values at later times were normalized by the earliest ($t \sim 5$ min) conductivity, σ_0 , as shown in Fig. 6b. According to Ha et al. [23], the presence of unburnt carbon in fly ash was found to cause an increase in electrical conductivity of concrete. In the present work, although the conductivity contribution from unburnt carbon in the RHAs is not known, given that there may be variability in the types of unburnt carbon present in each sample, normalization by σ_0 would relatively take into account such contribution. For each of the COM and GAS series, the conductivity drop becomes more dramatic, signifying increased pozzolanic activity, with lower burning temperature. This is in agreement with the trend in the amorphous SiO_2

content. From the overall rate of the conductivity drop, RHAs from the COM series show superior pozzolanic activity to those from the GAS series only at 600 °C and 750 °C of burning temperature. This finding is in accordance with the variation in the amorphous SiO_2 content, which is higher for the COM series than the GAS series only at 600 °C and 750 °C. Most surprisingly, COM 900 shows an increase in conductivity possibly due to the enhanced concentrations of Ca^{2+} and OH^- that dissolve into the solution at a faster rate than the rate at which they are consumed by the pozzolanic reaction, consistent with the lowest amorphous SiO_2 content (only $\sim 39\%$) of this RHA. An additional contribution to the increase in conductivity of the COM 900 might be from its highest equivalent alkali concentration as Na and K can dissolve rapidly into the solution as hydroxides and increase the conductivity. The decrease in conductivity after about 24 h of hydration for COM 900 might only be the result of the decreased ion mobility owing to drying water and thus is not related to the pozzolanic activity.

Towards quantification of pozzolanic activity, McCarter and Tran [19] identified four regions in the conductivity change when pulverized fly ash was mixed with $\text{Ca}(\text{OH})_2$ and water in paste form. Region I was characterized by the conductivity drop by about 10% of the initial value, pointing to some initial chemical reactivity on the particles. This drop was followed by a dormant period, associated with a very low rate of conductivity change in Region II. The most dramatic conductivity drop occurred in Region III, which was believed to correspond to the increase in rigidity of the paste due to setting. Lastly, in Region IV, the rate of the conductivity drop slowed down again. This slowing was attributed to the reduction in chemical activity when the sample became solid. They observed similar trends and regions for all other pozzolans in their study.

For the RHAs investigated in the present work, COM 600, GAS 600, and GAS 750 show only Regions III and IV, similar to the behavior of micro silica in the work of McCarter and Tran [19]. They reasoned that the rapid reaction that caused the absence of Region I and II (i.e., the

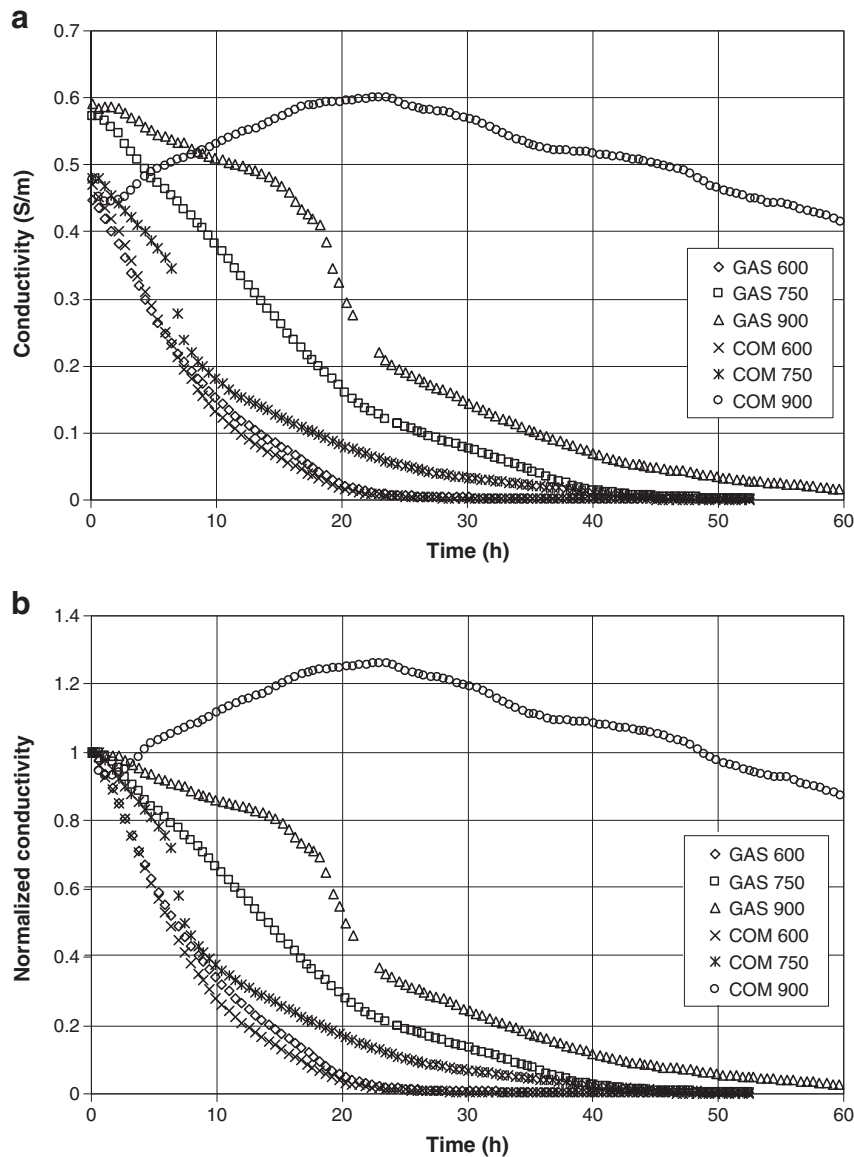


Fig. 6. Conductivity (a) and normalized conductivity (b) of the Ca(OH)_2 + RHA pastes.

immediate stiffening) in micro silica was due to its very high specific surface area. This observation also holds for COM 600, GAS 600, and GAS 750 in the present work, since they also possess very high specific surface areas and very high amorphous SiO_2 contents. On the other hand, COM 750 and GAS 900 show more than 10% conductivity drop in Region I, followed by a very steep drop in Region III and a slowing-down in Region IV. This behavior is similar to that of ground granulated blast furnace slag, as reported by McCarter and Tran [19]. The behavior of COM 900 (i.e., with increased conductivity) is, however, never encountered in their study.

The derivative of the normalized conductivity change, $d(\sigma/\sigma_0)/dt$, determined from Fig. 6b during the first 24 h of the Ca(OH)_2 + RHA pastes is shown in Table 2. The hydration time of 24 h is selected to minimize the influence of drying water, which seems to be pronounced after 24 h for most pastes. The amount of Ca(OH)_2 and CaCO_3 remaining in the pastes after 16 h of hydration from thermal analysis (TG and DTG) are also given in Table 2. (The authors originally hoped to obtain the amounts of Ca(OH)_2 and CaCO_3 after 24 h of hydration, in order to make a direct comparison to $d(\sigma/\sigma_0)/dt$ calculated over the first 24 h. However, the analysis only detected very minor amounts of the two compounds, so the hydration time was

reduced to only 16 h in hope of obtaining more significant amounts.) As suggested by Dweck et al. [22], the temperature ranges over which the decomposition of Ca(OH)_2 and CaCO_3 occurred were determined from the DTG curve of Fig. 7. Ca(OH)_2 was found to decompose into CaO and H_2O in the range 400–470 °C, while CaCO_3 decomposed into CaO and CO_2 in the broader range of 490–800 °C. Then, the weight losses due to such decompositions were determined from the TG

Table 2

$d(\sigma/\sigma_0)/dt$ during the first 24 h of hydration of the Ca(OH)_2 + RHA pastes, along with the corresponding amount of Ca(OH)_2 and CaCO_3 measured by thermal analysis (TG and DTG) after the pastes undergo 16 h of hydration.

	$d(\sigma/\sigma_0)/dt$ $t=0-24$ h (h^{-1})	Ca(OH)_2 content (% ignited weight)	CaCO_3 content (% ignited weight)
GAS 600	-4.018×10^{-2}	4.05	12.83
GAS 750	-3.623×10^{-2}	4.45	7.76
GAS 900	-2.364×10^{-2}	7.14	9.12
COM 600	-4.028×10^{-2}	6.79	5.09
COM 750	-3.935×10^{-2}	7.98	2.46
COM 900	1.513×10^{-2}	9.17	1.61

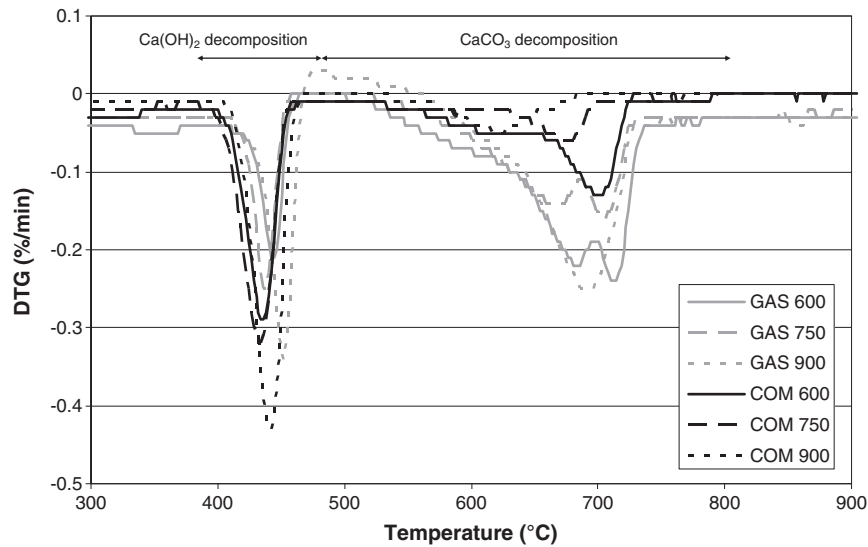


Fig. 7. DTG curves of the Ca(OH)_2 + RHA pastes at approximately 16 h of hydration. The peak over 400–470 °C corresponds to the decomposition of Ca(OH)_2 into CaO and H_2O ; the broader peak over 490–800 °C corresponds to the decomposition of CaCO_3 into CaO and CO_2 .

curve of Fig. 8, whose inset shows, for instance, the weight losses due to Ca(OH)_2 decomposition for the different pastes. (Although not shown, the weight losses due to CaCO_3 decomposition were determined in the same manner.) For a more careful estimation, the Ca(OH)_2 and CaCO_3 contents were calculated with respect to the final ignited weight of the pastes at 1000 °C, as recommended by Taylor [24].

From Table 2, for each of the COM and GAS series, the slope $d(\sigma/\sigma_0)/dt$ agrees well with the variation in the Ca(OH)_2 content; the sharper slope corresponds to the smaller amount of Ca(OH)_2 remaining (i.e., the more amount consumed by the pozzolanic reaction). However, when the two series are considered all together, the comparison grows more problematic. For examples, COM 750 seems to consume less Ca(OH)_2 , although its slope is much sharper, than GAS 900, or the sharpest slope in COM 600 is not associated with the least Ca(OH)_2 remaining. The main factor preventing comparison across the COM and GAS series might be the vast difference in the unburnt carbon content between the two series. The unburnt carbon must play a vital role in converting a large amount of Ca(OH)_2 into

CaCO_3 , probably through carbonation during the high-temperature environment of the thermal analysis itself. This is confirmed by the significantly higher CaCO_3 contents detected for the GAS series in Table 2, despite the fact that the initial CaCO_3 contents, shown as “CaO” in the chemical oxide composition of Table 1, are not significantly different between the two series. Therefore, since Ca(OH)_2 is consumed by both the carbonation and pozzolanic reactions, especially in the GAS series, it might not be a proper indicator for the measure of pozzolanic activity and thus does not agree well with the slope $d(\sigma/\sigma_0)/dt$ when comparison is made across the two series.

To examine how the slope $d(\sigma/\sigma_0)/dt$ is influenced by the physical properties (namely, the amorphous SiO_2 content, the unburnt carbon content, and the specific surface area) of the RHA, the correlation coefficients between the slope and each of the three factors are shown in Table 3. The correlation coefficients are calculated for each of the COM and GAS series separately, and also for the overall results. The slope $d(\sigma/\sigma_0)/dt$ correlates very strongly with the amorphous SiO_2 content of the RHA, both when the two series are considered separately and overall. The remarkable linearity of the relationship

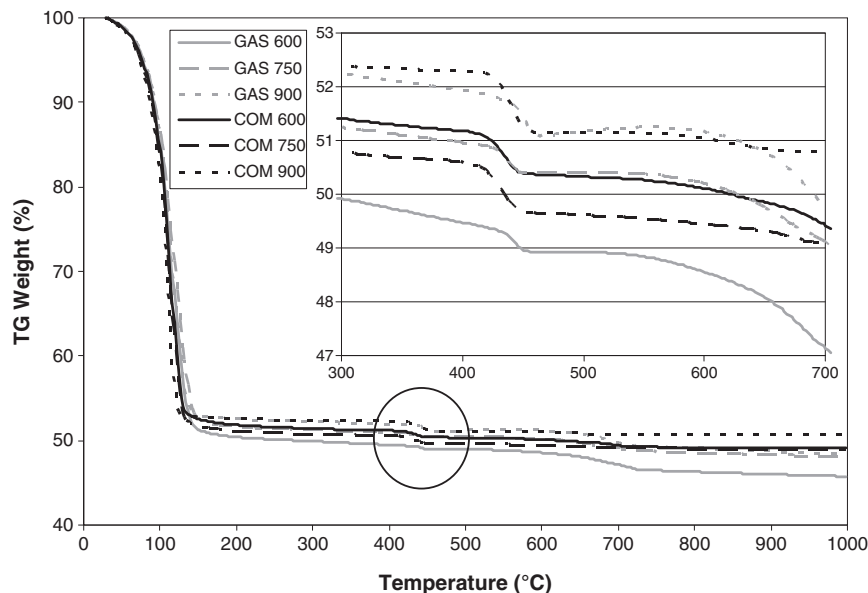


Fig. 8. TG curves of the Ca(OH)_2 + RHA pastes at approximately 16 h of hydration. The inset shows the weight losses due to decomposition of Ca(OH)_2 .

Table 3

Correlation coefficients between the slope $d(\sigma/\sigma_0)/dt$ and other properties of the RHAs, for the COM and GAS series, separately and overall.

	COM series	GAS series	Overall
Amorphous SiO ₂	−0.997	−0.986	−0.972
Carbon content	−0.259	0.996	−0.249
Specific surface area	−0.820	−0.817	−0.578
3-day strength activity index	−0.923	−0.995	−0.738
7-day strength activity index	−0.980	−0.926	−0.781
28-day strength activity index	−0.940	−0.845	−0.709

is displayed in Fig. 9. In Fig. 10, the linear relationship between the slope $d(\sigma/\sigma_0)/dt$ and the unburnt carbon content is observed only for the GAS series, confirming the vast difference in the correlation coefficients for each of the two series in Table 3. This finding indicates that the change in the slope $d(\sigma/\sigma_0)/dt$ for the GAS series is very strongly governed by the unburnt carbon content, while that of the COM series is not at all influenced by the unburnt carbon content. The observation is not surprising when taking into account the very minute unburnt carbon contents in the COM series. Apparently, the unburnt carbon content must be sufficiently high in order for its effect on the pozzolanic activity or the slope $d(\sigma/\sigma_0)/dt$ to be realized. Lastly, the correlation coefficients between the slope $d(\sigma/\sigma_0)/dt$ and the specific surface area for each of the two series are both quite respectable, as shown by the loose linearity in Fig. 11. (The authors are quite aware that the exact relationship between the slope $d(\sigma/\sigma_0)/dt$ and the specific surface area may not be linear. The lines in Fig. 11 are drawn only to facilitate the following discussion.) However, when both series are considered together, the overall correlation coefficient falls significantly. This drop might be an indication that since the specific surface area for the two series comes from quite different origins, they should be considered separately when compared to the pozzolanic activity or the slope $d(\sigma/\sigma_0)/dt$. For the COM series, with very low unburnt carbon content, the specific surface area results mainly from the amorphous SiO₂ content. However, the 6–8 wt.% unburnt carbon content in the GAS series can increase the specific surface area significantly, in addition to the contribution from the amorphous SiO₂ content. Therefore, since the increased specific surface area in the GAS series can act to both reduce (if resulting from the unburnt carbon content) and enhance (if resulting from the amorphous SiO₂ content) the pozzolanic activity, the slope $d(\sigma/\sigma_0)/dt$ for the GAS series is not as strong a function of the specific surface area as that of the COM series. This is confirmed by the steep slope (-5×10^{-4}) for COM and the much flatter slope (-8×10^{-5}) for GAS in Fig. 11.

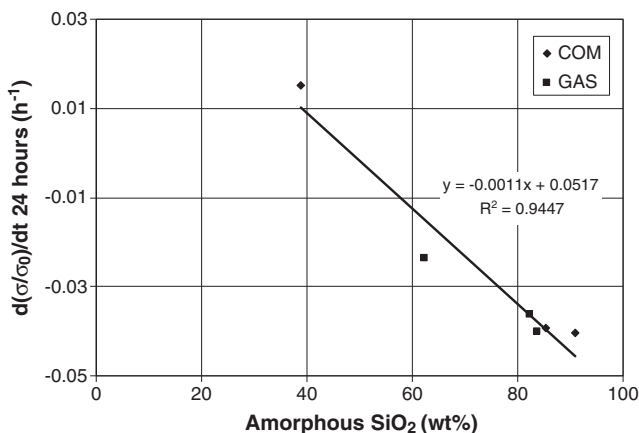


Fig. 9. Amorphous SiO₂ content of the RHA and the slope $d(\sigma/\sigma_0)/dt$ during the first 24 h of hydration of the Ca(OH)₂ + RHA pastes.

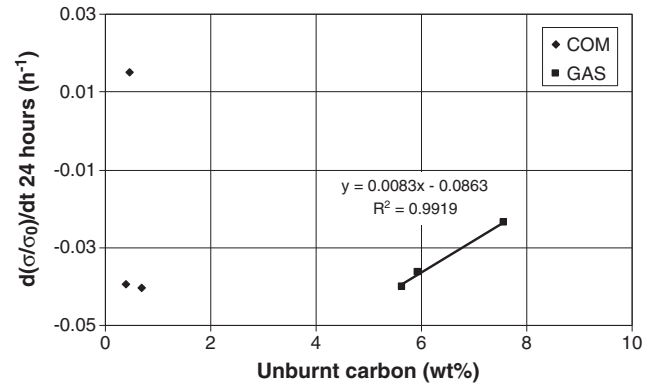


Fig. 10. Unburnt carbon content of the RHA vs. slope $d(\sigma/\sigma_0)/dt$ during the first 24 h of hydration of the Ca(OH)₂ + RHA pastes.

The correlation coefficients between the slope $d(\sigma/\sigma_0)/dt$ and the strength activity indices are shown at the bottom of Table 3. At all three ages, the correlation coefficients are exceptionally high when the two series are considered separately, but are significantly reduced when they are considered together. This trend, again, points to the limitation of using the slope $d(\sigma/\sigma_0)/dt$ obtained from impedance spectroscopy to assess pozzolanic activity. The method is especially sensitive to the amorphous SiO₂ and unburnt carbon contents and can serve as a very powerful tool for evaluating pozzolanic activity of RHA. However, the user must be careful not to apply the method to a group of RHAs with vastly different unburnt carbon contents.

4. Conclusions

The derivative of the normalized conductivity change, $d(\sigma/\sigma_0)/dt$, obtained from impedance spectroscopy during the first 24 h of hydration of the Ca(OH)₂ + RHA pastes can be used to evaluate the pozzolanic activity of RHA. The measurement proves to be sensitive to the unburnt carbon content in the range 6–8 wt.%, and especially sensitive to the amorphous SiO₂ content, regardless of the unburnt carbon content. It provides very high correlation coefficients to the strength activity index at all three ages considered when used to evaluate two separate groups of RHAs, each with comparable unburnt carbon contents. However, the correlation coefficients are significantly reduced when the RHAs with vast difference in the unburnt carbon contents are considered together. This points to the limitation in applying the method to evaluate the pozzolanic activity of RHA with vastly different carbon contents.

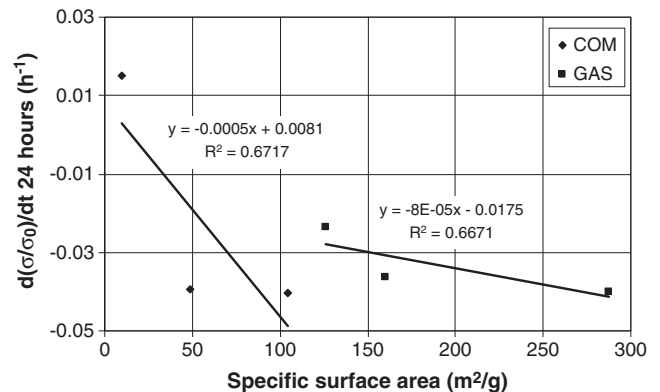


Fig. 11. Specific surface area of the RHA vs. slope $d(\sigma/\sigma_0)/dt$ during the first 24 h of hydration of the Ca(OH)₂ + RHA pastes.

Acknowledgement

The authors are grateful to Siam Research and Innovation Co. Ltd., Thailand, for the financial support and for providing the samples analyzed in this work.

References

- [1] S. Mindess, J.F. Young, D. Darwin, *Concrete*, Second ed., Prentice Hall, New Jersey, 2003.
- [2] T.M. Pounds, CO₂ abatement in cement and concrete 1990–2050, U.S. Environment Protection Agency's Resource Conservation Challenge Workshop, Washington D.C., USA, 2009.
- [3] P.K. Mehta, P.J.M. Monteiro, *Concrete Microstructure, Properties, and Materials*, Third ed., McGraw-Hill, New York, 2006.
- [4] Thailand Ministry of Energy website, Department of Alternative Energy Development and Efficiency, October 30, 2008, <http://www.alternative.in.th/index.php?option=com_content&view=article&id=232&Itemid=104> (Accessed February 2010).
- [5] P. Stroven, D.D. Bui, E. Sabuni, Ash of vegetable waste used for economic production of low to high strength hydraulic binders, *Fuel* 78 (1999) 153–159.
- [6] P.K. Mehta, Siliceous ashes and hydraulic cements prepared therefrom, U.S. Patent 4105459, 1978.
- [7] M. Nehdi, J. Duquette, A.E. Damatty, Performance of rice husk ash produced using a new technology as a mineral admixture in concrete, *Cement and Concrete Research* 33 (2003) 1203–1210.
- [8] D.G. Nair, K.S. Jagadish, A. Fraaij, Reactive pozzolanas from rice husk ash: an alternative to cement for rural housing, *Cement and Concrete Research* 36 (2006) 1062–1071.
- [9] J. Payá, M.V. Borrachero, J. Monzó, E. Peris-Mora, F. Amahjour, Enhanced conductivity measurement techniques for evaluation of fly ash pozzolanic activity, *Cement and Concrete Research* 31 (2001) 41–49.
- [10] A. Goldman, A. Bentur, The influence of microfillers on enhancement of concrete strength, *Cement and Concrete Research* 23 (1993) 962–972.
- [11] C. Real, M.D. Alcalá, J.M. Criado, Preparation of silica rice husks, *Journal of the American Ceramic Society* 79 (1996) 2012–2016.
- [12] M.I. Sánchez de Rojas, J. Rivera, M. Frías, Influence of microsilica state on pozzolanic reaction rate, *Cement and Concrete Research* 29 (1999) 945–949.
- [13] ASTM C311-04, Standard Test Methods for Sampling and Testing Fly Ash or Natural Pozzolans for Use in Portland-Cement Concrete, ASTM International, West Conshohocken, PA, 2004, pp. 204–212.
- [14] Spanish Standard, UNE 80225:1993 Ex, Métodos de ensayo de cementos. Análisis Químico, Determinación del dióxido de silicio (SiO₂) reactivo en los cementos, en las puzolanas y en las cenizas volantes, 1993.
- [15] Spanish Standard, UNE-EN 196-2:1996 Métodos de ensayo de cementos: Parte 2, Análisis Químico de cementos, 1996.
- [16] M.P. Luxán, F. Madruga, J. Saavedra, Rapid evaluation of pozzolanic activity of natural products by conductivity measurement, *Cement and Concrete Research* 19 (1989) 63–68.
- [17] C. Tashiro, K. Ikeda, Y. Inoue, Evaluation of pozzolanic activity by the electric resistance measurement method, *Cement and Concrete Research* 24 (1994) 1133–1139.
- [18] J. Payá, J. Monzó, M.V. Borrachero, A. Mellado, L.M. Ordoñez, Determination of amorphous silica in rice husk ash by a rapid analytical method, *Cement and Concrete Research* 31 (2001) 227–231.
- [19] W.J. McCarter, D. Tran, Monitoring pozzolanic activity by direct activation with calcium hydroxide, *Construction and Building Materials* 10 (1996) 179–184.
- [20] ASTM C109/C109M-02, Standard Test Method for Compressive Strength of Hydraulic Cement Mortars, ASTM International, West Conshohocken, PA, 2002, pp. 76–81.
- [21] R. Jaubertie, F. Rendell, S. Tamba, I. Cisse, Origin of the pozzolanic effect of rice husks, *Construction and Building Materials* 14 (2000) 419–423.
- [22] J. Dweck, P.M. Buchler, A.C.V. Coelho, F.K. Cartledge, Hydration of a Portland cement blended with calcium carbonate, *Thermochimica Acta* 346 (2000) 105–113.
- [23] T.-H. Ha, S. Muralidharan, J.-H. Bae, Y.-C. Ha, H.-G. Lee, K.W. Park, D.-K. Kim, Effect of unburnt carbon on the corrosion performance of fly ash cement mortar, *Construction and Building Materials* 19 (2005) 509–515.
- [24] H.F.W. Taylor, *Cement Chemistry*, First ed., Academic Press, London, 1990.